

**iScience, Volume 23**

**Supplemental Information**

**Inhibition of the Activity of Cyclophilin**

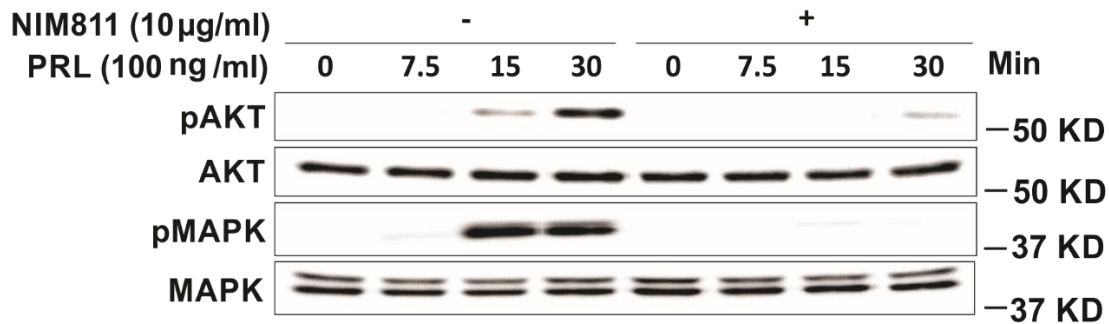
**A Impedes Prolactin Receptor-Mediated**

**Signaling, Mammary Tumorigenesis, and Metastases**

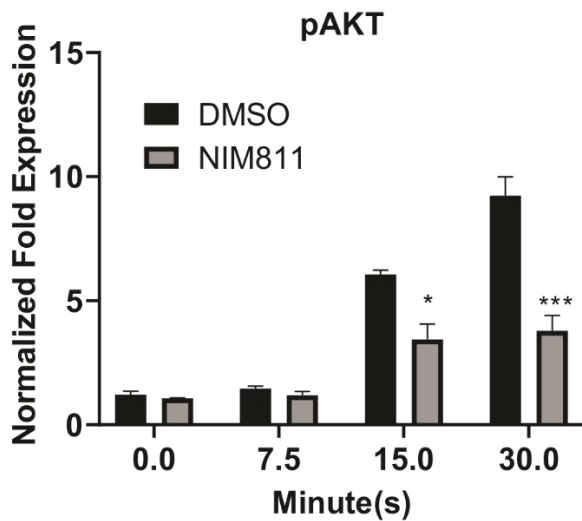
**Shawn Hakim, Justin M. Craig, Jennifer E. Koblinski, and Charles V. Clevenger**

## Supplemental Figures and Legends

**A.**



**B.**



**C.**

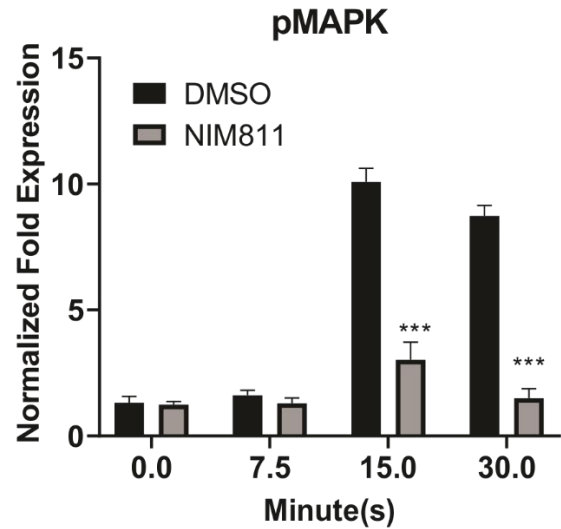


**Figure S1. NIM811 inhibits phosphorylation of AKT and MAPK, related to Figure 1.**

(A) T47D Cells were serum starved for 16-24 hours, pre-treated with NIM811 (10  $\mu\text{g/ml}$ ) for 4-6 hours and/or stimulated with PRL (250 ng/ml) at the indicated times. Blots were probed with the indicated antibodies. (B, C) Quantification of fold expression of phospho-proteins (pAKT and pMAPK) normalized to their respective total proteins in panel A as indicated. Quantification of blots in panel A. *Column*, mean of three independent experiments; *error bars*,  $\pm\text{SEM}$ . \* $P < 0.05$ , \*\*\* $P < 0.005$ . T-test was performed to determine significance.

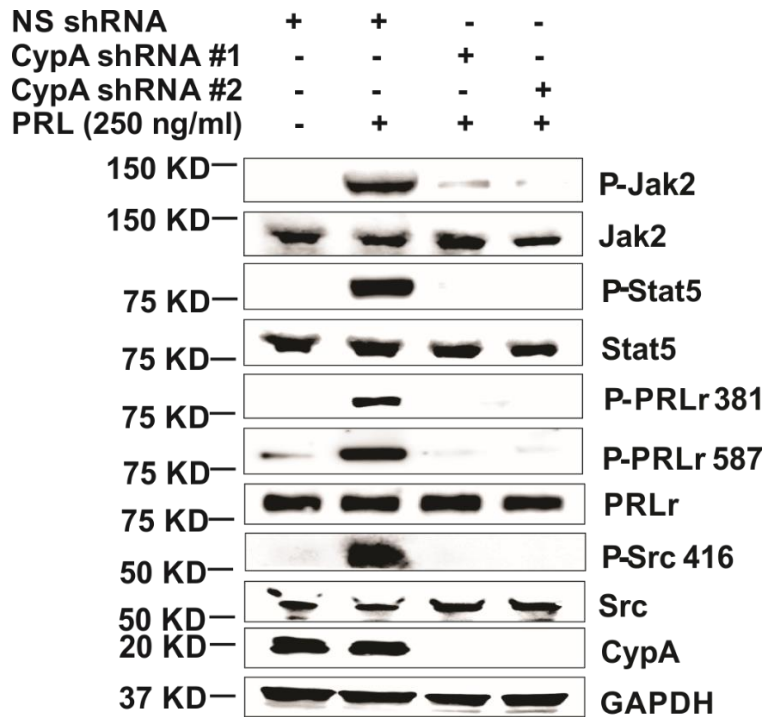


**Figure S2. Both shRNA sequences targeting CypA demonstrate effective knockdown of the protein and phosphorylation of signaling intermediates, related to Figure 2.** Stable expression of non-silencing control or CypA shRNA in T47D were serum starved for 16-24 hours, stimulated with PRL (250 ng/ml) for 15 minutes and blots were probed with the indicated antibodies.

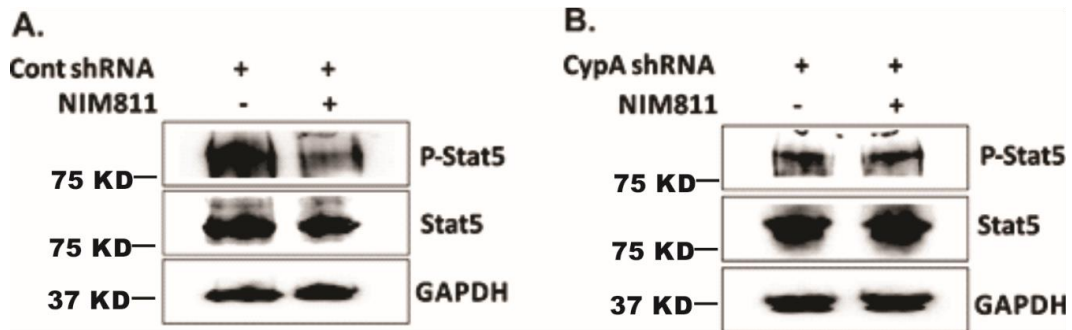


**Figure S3. NIM811 inhibits phosphorylation of Stat5 only in CypA-expressing cells, related to Figure 2. (A)** Stable expression of non-silencing control shRNA in T47D were serum starved for 16-24 hours, pre-treated with NIM811 for 4 hours and stimulated with PRL (250 ng/ml) for 15 minutes and blots were probed with the indicated antibodies. **(B)** Stable expression of CypA shRNA were treated as indicated above and blots were probed with indicated antibodies.

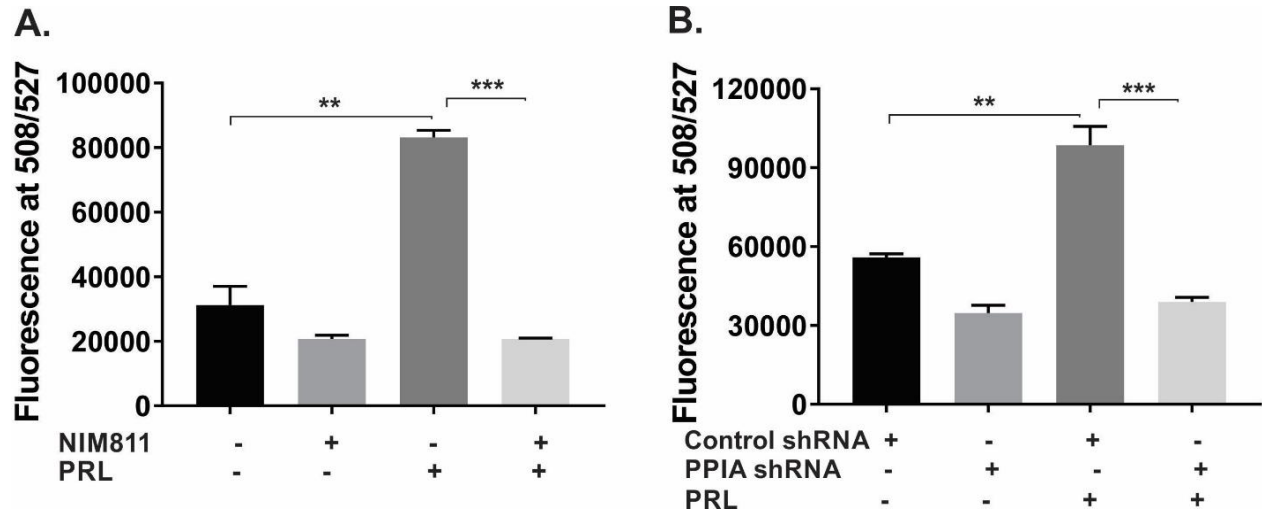


**Figure S4. Inhibition or knockdown of CypA significantly decreases breast cancer cell proliferation, related to Figure 5. (A & B)** Cell proliferation was measured by CyQuant (Thermo Fisher) proliferation assay. **(A)** Cells were pre-treated with NIM811 (10 ug/ml) and/or PRL (250 ng/ml). **(B)** Non-targeting control or CypA shRNA transfected in T47D cells and/or PRL (250 ng/ml). *Columns*, mean of three independent experiments; *error bars*,  $\pm$ SEM. \*\*P < 0.01, \*\*\*P < 0.005. One-way ANOVA with Tukey's test was used to determine significance.

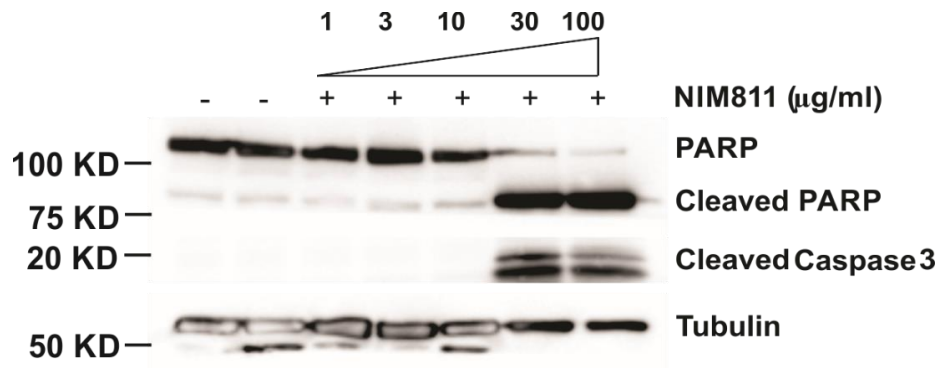


**Figure S5. Treatment of high dose of NIM811 induces apoptosis, related to Figure 5.** T47D cells were treated with various doses of NIM811 for 96 hours. Cell lysates were collected and immunoblotted with PARP or cleaved caspase 3 antibody as indicated.  $\alpha$ -Tubulin is used as the loading control.

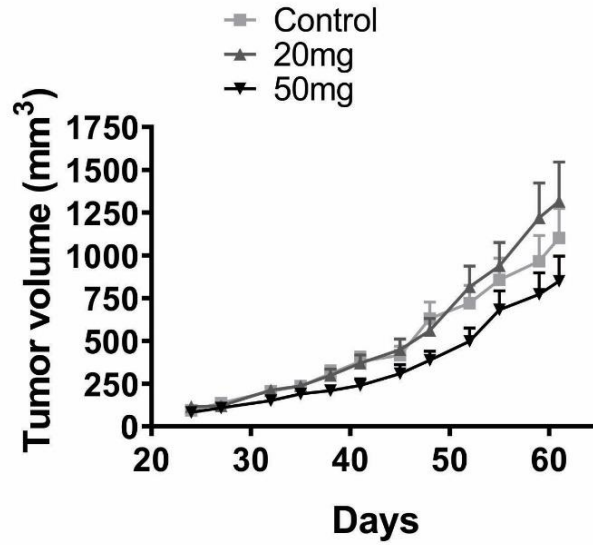


**Figure S6. NIM811 treatment does not alter tumor growth, related to Figure 7.** Quantification of primary tumor volume based on caliper measurements on the indicated days for each cohort. The difference in tumor volume between control vs. treatment(s) is not significant,  $P < 0.149$ . One-way ANOVA was used to determine significance.

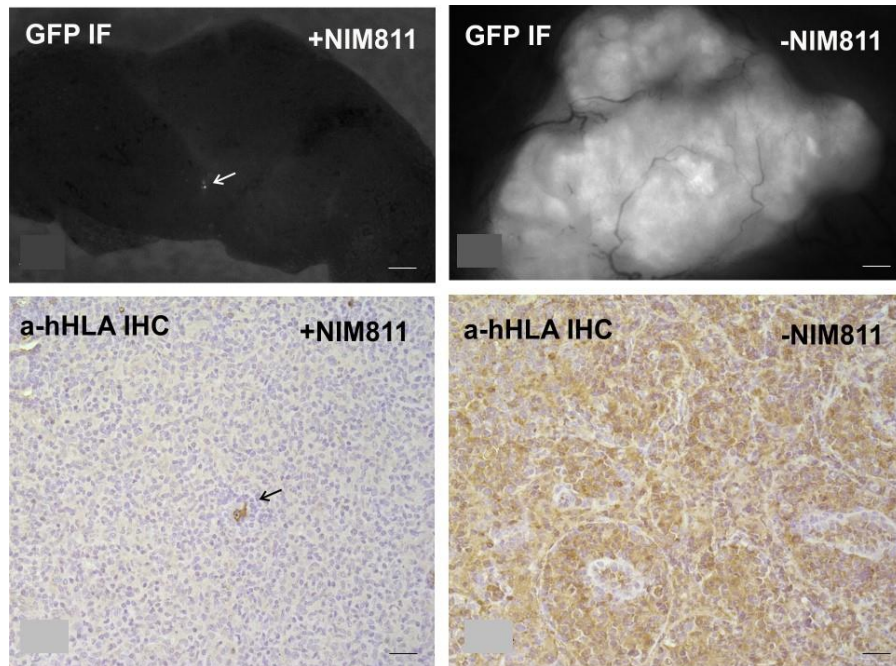


**Figure S7. NIM811 therapy prevents macrometastatic outgrowth in GFP-labeled MDA231 xenografts, related to Figure 7.** IF analyses for GFP label present in the xenografts treated 6 weeks with 50 mg/kg/day NIM811 (or carrier control; treatment initiated after 2 weeks of outgrowth) is presented in the upper panels, bar “\_” = 1 cm; IHC confirmation with a-human HLA1 antibody is seen in lower panels, bar “\_” = 100  $\mu$ m.



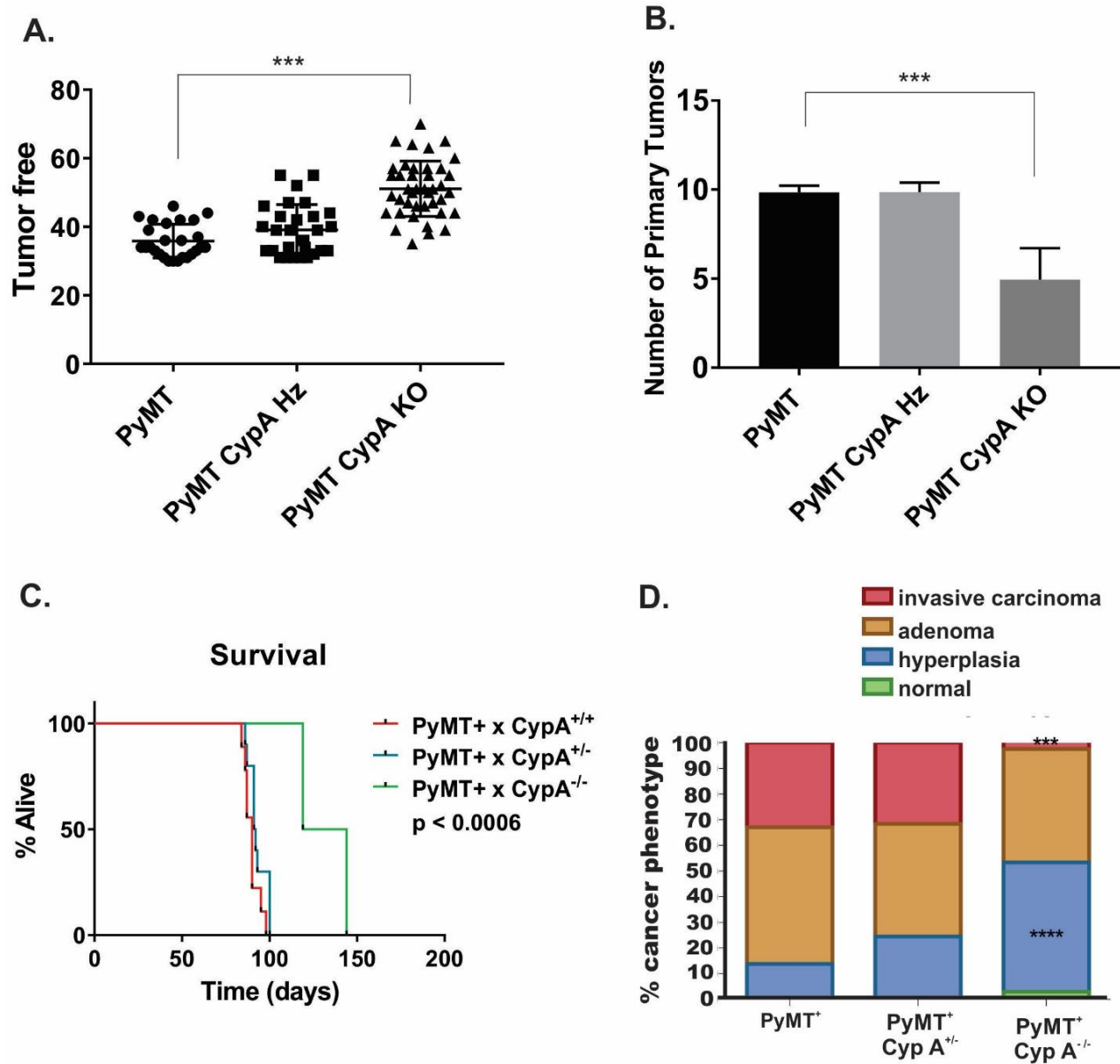


**Figure S8. CypA deletion markedly inhibits PyMT mammary tumorigenesis, related to Figure 8.** (A) CypA<sup>-/-</sup> x PyMT<sup>+</sup> mice demonstrate significantly delayed tumor latency (\*\*P < 0.005). One-way ANOVA with Dunnett's test was used to determine significance. (B) Compared to CypA<sup>+/+</sup> x PyMT<sup>+</sup>, CypA<sup>-/-</sup> x PyMT<sup>+</sup> mice demonstrate significantly reduced number of primary tumors (\*\*P < 0.005). One-way ANOVA with Dunnett's test was used to determine significance. (C) Kaplan-Meier plots of overall survival (P < 0.0006) reveal highly significant differences between CypA<sup>+/+</sup> and CypA<sup>-/-</sup> mice when

bred into the PyMT mouse model of mammary tumorigenesis. **(D)** Percent cancer phenotypes based on histological analysis under brightfield microscopy. Percent of total denotes the portion of FFPE mouse mammary gland H&E stained tissue sections exhibiting features of (1) invasive carcinoma, (2) adenoma, (3) hyperplasia, (4) normal mammary tissue. Statistics based upon an n = 12 for each cohort based upon comparison to WT (PyMT<sup>+</sup>) (\*\*\*\*p < 0.001). Two-way ANOVA with Dunnett's test for multiple comparisons and based upon comparison to WT(PyMT) was used to determine significance.

## **Transparent Methods**

### **Cell culture and reagent**

T47D and MDA 231 human breast cancer cell lines were obtained from ATCC (Manassas, VA) and cultured in Dulbecco's modified Eagles's medium supplemented with 10% fetal bovine serum, 100 U/ml penicillin and 100 µg/ml streptomycin (Life Technologies). All cells were incubated in a humidified 5% CO<sub>2</sub>/95% air atmosphere at 37°C. Human recombinant PRL was a gift from Dr. Anthony Kossiakoff (University of Chicago, Chicago, IL). PRL was added to cells to yield a final concentration of 250 ng/ml. N-methyl-4-isoleucine-cyclosporin (NIM811) was obtained from Novartis and pre-incubated for 2-4 hours prior to stimulation with PRL.

### **shRNA Constructs**

TripZ shRNA with mature antisense 5'-TAGGATGAAGTTCTCATCT-3' (V3THS\_304403) and 5'-TCTGCTGTCTTTGGGACCT-3' (V3THS\_304404) target sequences against PPIA (CypA) as well as non-targeting control shRNA controls were purchased from Dharmacon as glycerol stocks. Bacterial cultures were grown with Carbenicillin (100 µg/ml, Fisher Scientific) and subsequently plasmids were purified using EndoFree<sup>R</sup> Plasmid Maxi Kit (Qiagen) according to the manufacturer's instructions. Purified plasmid DNA were transfected in HEK 293T using Lipofectamine 3000 (Life Technologies) according to the manufacturer's instructions.

### **Antibodies**

Antibodies utilized for western blot analysis were obtained from the following sources and used as described: anti-pPRLr 381 (Custom antibody from New England Biolabs, 1:500), anti-pPRLr 587 (Custom antibody from New England Biolabs, 1:500), anti-PRLr (Life Technologies, 1:1000), anti-p-Jak2 1007/1008 (Cell Signaling Technology, 1:500), anti-Jak2 (Cell Signaling Technology, 1:1000), anti-pStat5 (Cell Signaling Technology, 1:1000), anti-Stat5 (Santa Cruz Biotechnology,

1:1500), anti-pSrc416 (Cell Signaling Technology, 1:500), anti-Src (Cell Signaling Technology, 1:1000), anti-CISH (Santa Cruz Biotechnology, 1:1000), anti-CyclinD1 (Santa Cruz Biotechnology, 1:1000), anti-Cyclophilin A (Santa Cruz Biotechnology, 1:1000), anti-GAPDH (Cell Signaling Technology, 1:2000), and anti-Tubulin (ABCAM, 1:1000) diluted in TBS-T with 3% milk or BSA as suggested by the specific manufacturer.

## **Experimental Methods**

### **Mouse MMTV-PyMT model**

For tumorigenesis studies, the well-recognized mouse model of transgene-driven tumorigenesis (Muller et al., 1988) utilizing the MMTV-driven expression of polyomavirus middle T in mouse mammary glands was employed. PyMT mice were purchased from The Jackson Laboratory (Jax; Stock # 002374, FVB/N-Tg(MMTV-PyVT)634Mul/J). Hemizygous males were cross-bred with our transgenic CypA<sup>-/-</sup> female mice (Volker et al., 2018) until a PyMT<sup>+</sup>/CypA<sup>+/-</sup> male mouse was obtained. This sire was then bred with the CypA<sup>-/-</sup> dams until PyMT<sup>+</sup>/CypA<sup>+/-</sup> and PyMT<sup>+</sup>/CypA<sup>-/-</sup> females were obtained for use in this study. Tumors were monitored beginning at weaning until time of dissection via palpating and calipering. Mice were kept in accordance to an approved IACUC protocol which allowed the humane endpoint of when any single tumor reached 17 mm in diameter. Dissection timepoints included 5 weeks (hyperplasia phase in PyMT model), 8 weeks (adenoma phase), 11 weeks (invasive carcinoma phase), and 13 weeks (distal metastasis phase). Mice were weighed and whole mammary glands containing tumors were calipered upon dissection. Lungs and lymph nodes were weighed and collected as well. Following fixation with 10% buffered neutral-buffered formalin, tumors were paraffin-embedded and processed for histologic and histochemical analyses.

## **Mouse xenograft model**

Four to six weeks old female nude mice were used for the xenograft study. To assess the effects of NIM811 on the xenograft growth, MDA231 cells ( $0.5 \times 10^6$ ) expressing mCherry fluorescent protein (Puchalapalli et al., 2016) were suspended in Matrigel and injected into the teat of the fourth abdominal mammary gland of nude mice as described (Harrell et al., 2006). When tumor volume reached 80-100 mm<sup>3</sup>, animals were randomized into three groups and were treated with vehicle control (olive oil) and NIM811 (20 mg/kg/day, 50 mg/kg/day) for 4 weeks by twice-daily gavages. Tumor growth was measured by weekly caliper measurement using the formula length  $\times$  breadth<sup>2</sup>/2. In the end of experiment, mice were sacrificed. The entire primary mammary tumors were removed and weighed. In addition, all visceral organs, bones, brain, and superficial lymph nodes were harvested for microscopic examination for metastasis. Metastases were detected by the presence of mCherry fluorescent protein using Zeiss StereoDiscovery. V12 fluorescence dissecting microscope with an AxioCam MRm digital camera. One half of each tumor and other organs were fixed, embedded, sectioned, and stained with H&E. The necrotic area of primary tumor was quantified by morphometric determination of the proportion of total tumor area that was necrotic in H&E staining section.

## **Method Details**

### **Western blotting and analysis**

Cell lysates were analyzed by western blot analysis as previously described in (Zheng et al., 2008). Cells were grown in 100 cm<sup>2</sup> dishes until 70%-80% confluence followed by starvation for 16-24 hrs before PRL treatment (100 ng/ml) in conditioned media (DMEM, Life Technologies). Cells were lysed in RIPA buffer and cell lysates were blotted by specific antibodies as listed in the key resources section. Target proteins were visualized by enhanced chemiluminescence (GE

Healthcare), and images were captured using Fujifilm LAS-3000 system. The band intensities were quantified by LAS-3000 analysis tools and normalized to those of their respective loading control bands. Data were expressed as fold changes compared with an appropriate control.

### **Lentivirus production and transduction**

Transfection of TripZ shRNA or control shRNA was performed with necessary components to produce/collect virus 48 hours post-transfection according to Dharmacon protocol/kit. T47D cells were infected with filtered virus and puromycin selected 48 hours post infection according to Dharmacon instructions. Following antibiotic selection, Doxycycline at a concentration of 1  $\mu$ g/ml was used for induction of TurboRFP/shRNA expression.

### **Cell viability**

Trypan blue exclusion method as described (Strober, 2001) was used to assess cell viability.  $1 \times 10^5$  cells were plated and cultured for 24 hours, and then serum starved for overnight. Cells were treated with PRL and/or NIM811 in indicated concentrations for the indicated timepoints. DMEM, along with trypsinized cells were centrifuged at 200 x g, and then resuspended in PBS and Trypan blue. Cells were counted on a Countess Automated Cell Counter (Invitrogen) and percentage of live cells was calculated. Cell viability was measured in the same manner for duration of the experiment.

### **Wound healing assay**

MDA231 and T47D confluent cell monolayers was wounded with a p200 pipette tip and cultured in serum-free medium in the presence of various concentrations of NIM811. Representative images of a wound closure assay were acquired with a phase-contrast microscope at indicated times. The wound areas were measured using Image J and the percentage of the wound closed was calculated.

### **Boyden chamber migration assay**

MDA231 and T47D cells were placed in the top of a trans-well chamber with 8  $\mu\text{m}$  pore polyethylene terephthalate (PET) membranes in the presence of various doses of NIM811. Serum free media (SFM) with 2% FBS medium were placed in the bottom of the chamber. After 24 hours, the number of cells migrating to the lower surface of the membrane was quantified by CyQuant<sup>TM</sup> (Invitrogen).

### **Soft agar colony formation assay**

A bottom agar was prepared by solidifying 1 mL of 0.8% SeaPlaque agarose (BioWhitaker) in 10 % FBS-containing growth media in each well of a 6-well plate. The bottom agar was overlaid with 800  $\mu\text{l}$  of a 0.45% top agar mixture containing 10,000 cells per well in the presence of various concentration of NIM811. The plates were incubated at 37°C for 14 (MDA231 cells) to 21 (T47D cells) days, colonies were counted using a light microscope with an ocular grid. Only colonies ( $\geq 50 \mu\text{m}$ ) were counted with Image J software. Five random fields were counted for each well and the average number of colonies per well is shown.

### **RNA extraction, cDNA synthesis, and qRT-PCR**

T47D cells were plated in 10 cm plate as described in the later section and treated with DMSO (0.1%) control, PRL (250 ng/mL in 0.1% DMSO), and/or NIM811 (10  $\mu\text{g}/\text{ml}$  in 0.1% DMSO). After treatments, cells were washed with PBS and mRNA was isolated with a PureLink<sup>TM</sup> RNA Mini Kit (Invitrogen/Fisher Scientific) according to manufacturer's instructions. cDNA was synthesized using 1  $\mu\text{g}$  of total mRNA with iScript<sup>TM</sup> Reverse Transcription Supermix (BioRad) according to the manufacturer's protocol. qPCR was performed using iTaq<sup>TM</sup> Universal SYBR<sup>R</sup> Green Supermix (Biorad), 20 ng of DNA, and 1 nmol/L primers as follows: CCND1 forward 5'- CCGTCCATGCGGAAGATC-3', reverse 5'- GAAGACCTCCTCCTCGCACTT-3'; CISH

forward 5'- AGAGGAGGATCTGCTGTGCAT-3', reverse 5'-  
GGAACCCCAATACCAGCCAG; GAPDH forward 5'- CATGAGAAGTATGACAACAGCCT-  
3', Reverse 5'- AGTCCTTCCACGATACCAAAGT-3' using a BioRad CFX96 Real-Time PCR  
thermocycler. Data were normalized to GAPDH and fold change were represented as  $2^{-\Delta\Delta C_t}$  ( $2^{-(C_t\text{Target}-C_t\text{GAPDH})\text{PRL}-(C_t\text{Target}-C_t\text{GAPDH})\text{Control}}$ ) using untreated DMSO control as baseline.

### **Cell culture and RNA Isolation for microarray**

Differential gene expression was assessed in T47D cells treated with DMSO (0.1%) control, PRL (250 ng/mL in 0.1% DMSO), and/or NIM811 (10 ug/ml in 0.1% DMSO). Prior to RNA isolation, T47D cells were plated at 60% confluency in 10-cm plates and incubated for 24 hours in complete media followed by an additional 24 hours of serum starvation in DMEM (Life Technologies) and 1X ITS Liquid Media Supplement (Sigma Aldrich). Cells were then treated for 4 hours with either DMSO or NIM811 before stimulation with PRL. After 2-hour PRL stimulation, cells were washed with PBS and RNA was extracted using the MagMAX-96 for Microarrays Total RNA Isolation Kit (Invitrogen, Life Technologies) in an automated fashion using the magnetic particle processors MagMAX Express. RNA purity was judged by spectrophotometry at 260, 270, and 280 nm. RNA integrity was assessed by running 1  $\mu$ l of every sample in RNA 6000 Nano LabChips on the 2100 Bioanalyzer (Agilent Technologies).

### **Microarray hybridization and Data Acquisition**

Each of the four cell treatment conditions (PRL<sup>-</sup>/DMSO, PRL<sup>+</sup>/DMSO, PRL<sup>-</sup>/NIM811, PRL<sup>+</sup>/NIM811) were assessed in three independently grown biological replicates. Each of the 12 RNA samples were hybridized in duplicate to two Human Genome U133A 2.0 Arrays (Affymetrix, Santa Barbara, CA) according to the Affymetrix protocol as previously described (Dumur et al., 2004) with modifications : Starting with 500 ng of total RNA, we performed a



single-strand cDNA synthesis primed with a T7-(dT24) oligonucleotide. Second strand cDNA synthesis was performed with *E. coli* DNA Polymerase I, and biotinylation of the cRNA was achieved by in vitro transcription (IVT) reaction using the GeneChip 3' IVT Express Kit (Affymetrix, Santa Clara, CA). After a 37°C-incubation for 16 hours, the labeled cRNA was purified using the cRNA cleanup reagents from the GeneChip Sample Cleanup Module. As per the Affymetrix protocol, 10 µg of fragmented cRNA were hybridized on the GeneChip HG U133A 2.0 Arrays (Affymetrix Inc., Santa Clara, CA) for 16 hours at 60 rpm in a 45 °C hybridization oven. The arrays were washed and stained using the GeneChip Hybridization, Wash, and Stain Kit in the Affymetrix fluidics workstation. Every chip was scanned at a high resolution, on the Affymetrix GeneChip Scanner 3000 7G according to the GeneChip Expression Analysis Technical Manual procedures (Affymetrix, Santa Barbara, CA). After scanning, the raw intensities for every probe were stored in electronic files (in *.DAT* and *.CEL* formats) by the GeneChip Operating Software v1.4 (GCOS) (Affymetrix, Santa Barbara, CA).

## **Histology**

All mammary glands, lymph nodes, and lungs were fixed in 10% neutral buffered formalin (NBF) for 24-48 hours, depending on the size of the tumor, and then stored in 70% ethanol at 4 degrees. All tissues were processed together to form FFPE blocks and sectioned into 5 µm thick sections by the VCU Cancer Mouse Models Core laboratory as well as Anatomic Pathology Research Services at VCU Health for histological analysis by hematoxylin, gill no. 3 (cat. # GHS332, Sigma Aldrich, St. Louis, MO) and eosin Y (cat. # 318906, Sigma Aldrich, St. Louis, MO) staining as described (Volker et al., 2018). Positivity of lymph nodes was determined as lymph nodes containing at least 1 macro-metastasis. FFPE hematoxylin and eosin stained axillary and accessory axillary lymph nodes were assessed for presence of metastases by Dr. C.V. Clevenger, a board-

certified pathologist, under brightfield microscopy. Slides were then imaged with the NanoZoomer RS Digital Slide Scanner (Hamamatsu Photonics, Bridgewater, NJ) and analyzed using utilizing NDPview2 software (Hamamatsu Photonics). Lung metastases were counted, and borders of metastases drawn as free ROIs in this software. The software calculated a scaled area from the scanned image metadata. Areas of each metastasis as well as each lung lobe were totaled for each mouse. The metastasis area was normalized to total lung area and expressed as a percent to account for the anatomical size difference of the organs between the WT and KO mice (Volker et al., 2018).

## **Quantification and Statistical Analysis**

### **Differential Expression Analysis**

The 12 resultant *.CEL* files were analyzed using the R statistical computing language and environment (RDevelopmentCoreTeam, 2011). The data quality of each microarray was assessed by examining the average background, percent of probe sets called present by the MAS5 detection call algorithm (Gautier et al., 2004), and the 3':5' ratio for GAPDH and ACTIN. Additionally, to detect potential spatial artifacts resulting from sub-optimal hybridization conditions, probe level linear models were fit using the R Bioconductor package, “affyPLM”, and plots of the residuals were examined for each microarray (Bolstad et al., 2004; Gentleman et al., 2004). Differential expression was assessed using the “affy” and “limma” Bioconductor packages (Gautier et al., 2004; Smyth, 2004). Briefly, probesets were quantile normalized and processed by the Robust Multi-Array Average (RMA) algorithm (Irizarry et al., 2003) before the manufacturer’s control probesets and probesets considered “absent” in 20 or more arrays by the MAS5 algorithm were filtered from all arrays (Archer and Reese, 2010). Differential expression between treatment conditions was then assessed via moderated t-test adjusted for multiple hypotheses by the

Benjamini & Hochberg method (Benjamini and Hochberg, 1995). The false discovery rate (FDR) was controlled so that only those probesets with  $q < 0.01$  were deemed significant.

Hierarchical clustering was performed on the top 100 prolactin induced and top 100 prolactin inhibited genes (as defined by the expression fold change between the PRL<sup>+</sup> / DMSO and PRL<sup>-</sup> / DMSO microarrays) utilizing the GenePattern public server (de Hoon et al., 2004; Eisen et al., 1998; Reich et al., 2006). Microarrays were clustered using a pairwise average-linkage method and Pearson correlation as the similarity metric; genes were not subjected to clustering and are presented as originally ordered in the *.GCT* file supplied to the module.

STAT5 target genes were defined as previously reported (Kang et al., 2014) and include genes flanked by the classic STAT5 palindromic repeat binding motif as well as those identified by Kang et al. utilizing STAT5 ChIP-seq on murine mammary tissues at parturition. After converting *Mus musculus* gene annotations to human gene symbols, 847 unique genes comprised the STAT5 target gene list used in this study.

### **Statistical Analysis**

Statistical analysis was performed using appropriate statistical methods including Student t-test, one- and two-way ANOVA and parametric tests using GraphPad Prism V7.0g (GraphPad Software, Inc.) and JMP version 12.0. The data are shown as the mean with error bars showing  $\pm$  SEM. Statistical significance indicated as \*P < 0.05, \*\*P < 0.01, \*\*\* P < 0.005 and \*\*\*\*P < 0.001.

### **Study Approval**

Animals were housed in conventional or pathogen-free conditions, where appropriate, at the mouse facility of Virginia Commonwealth University, in compliance with Institutional Animal Care and Use Committee (IACUC) regulations. All animal experiments were performed according to

protocols approved by the Animal Care and Use Committee of the Virginia Commonwealth University.

## Supplemental References

- Archer, K.J., and Reese, S.E. (2010). Detection call algorithms for high-throughput gene expression microarray data. *Brief Bioinform* *11*, 244-252.
- Benjamini, Y., and Hochberg, Y. (1995). Controlling the False Discovery Rate - a Practical and Powerful Approach to Multiple Testing. *J Roy Stat Soc B Met* *57*, 289-300.
- Bolstad, B.M., Collin, F., Simpson, K.M., Irizarry, R.A., and Speed, T.P. (2004). Experimental design and low-level analysis of microarray data. *Int Rev Neurobiol* *60*, 25-58.
- de Hoon, M.J., Imoto, S., Nolan, J., and Miyano, S. (2004). Open source clustering software. *Bioinformatics* *20*, 1453-1454.
- Dumur, C.I., Nasim, S., Best, A.M., Archer, K.J., Ladd, A.C., Mas, V.R., Wilkinson, D.S., Garrett, C.T., and Ferreira-Gonzalez, A. (2004). Evaluation of quality-control criteria for microarray gene expression analysis. *Clin Chem* *50*, 1994-2002.
- Eisen, M.B., Spellman, P.T., Brown, P.O., and Botstein, D. (1998). Cluster analysis and display of genome-wide expression patterns. *Proc Natl Acad Sci U S A* *95*, 14863-14868.
- Gautier, L., Cope, L., Bolstad, B.M., and Irizarry, R.A. (2004). affy - analysis of Affymetrix GeneChip data at the probe level. *Bioinformatics* *20*, 307-315.
- Gentleman, R.C., Carey, V.J., Bates, D.M., Bolstad, B., Dettling, M., Dudoit, S., Ellis, B., Gautier, L., Ge, Y., Gentry, J., *et al.* (2004). Bioconductor: open software development for computational biology and bioinformatics. *Genome Biol* *5*, R80.
- Harrell, J.C., Dye, W.W., Allred, D.C., Jedlicka, P., Spoelstra, N.S., Sartorius, C.A., and Horwitz, K.B. (2006). Estrogen receptor positive breast cancer metastasis: altered hormonal sensitivity and tumor aggressiveness in lymphatic vessels and lymph nodes. *Cancer Res* *66*, 9308-9315.
- Irizarry, R.A., Bolstad, B.M., Collin, F., Cope, L.M., Hobbs, B., and Speed, T.P. (2003). Summaries of Affymetrix GeneChip probe level data. *Nucleic Acids Res* *31*, e15.
- Kang, K., Yamaji, D., Yoo, K.H., Robinson, G.W., and Hennighausen, L. (2014). Mammary-Specific Gene Activation Is Defined by Progressive Recruitment of STAT5 during Pregnancy and the Establishment of H3K4me3 Marks. *Mol Cell Biol* *34*, 464-473.
- Muller, W.J., Sinn, E., Pattengale, P.K., Wallace, R., and Leder, P. (1988). Single-step induction of mammary adenocarcinoma in transgenic mice bearing the activated c-neu oncogene. *Cell* *54*, 105-115.

Puchalapalli, M., Zeng, X., Mu, L., Anderson, A., Hix Glickman, L., Zhang, M., Sayyad, M.R., Mosticone Wangenstein, S., Clevenger, C.V., and Koblinski, J.E. (2016). NSG Mice Provide a Better Spontaneous Model of Breast Cancer Metastasis than Athymic (Nude) Mice. *PLoS One* 11, e0163521.

RDevelopmentCoreTeam (2011). *R: A Language and Environment for Statistical Computing* (Vienna, Austria: The R Foundation for Statistical Computing).

Reich, M., Liefeld, T., Gould, J., Lerner, J., Tamayo, P., and Mesirov, J.P. (2006). GenePattern 2.0. *Nat Genet* 38, 500-501.

Smyth, G.K. (2004). Linear models and empirical bayes methods for assessing differential expression in microarray experiments. *Stat Appl Genet Mol Biol* 3, Article3.

Strober, W. (2001). Trypan blue exclusion test of cell viability. *Curr Protoc Immunol Appendix* 3, Appendix 3B.

Volker, S.E., Hedrick, S.E., Feeney, Y.B., and Clevenger, C.V. (2018). Cyclophilin A Function in Mammary Epithelium Impacts Jak2/Stat5 Signaling, Morphogenesis, Differentiation, and Tumorigenesis in the Mammary Gland. *Cancer Res* 78, 3877-3887.

Zheng, J., Koblinski, J.E., Dutson, L.V., Feeney, Y.B., and Clevenger, C.V. (2008). Prolyl isomerase cyclophilin A regulation of Janus-activated kinase 2 and the progression of human breast cancer. *Cancer Res* 68, 7769-7778.